

BIODYNAMIC VERIFICATION OF AN ESTIMATED MUSCULAR ACTIVITY MODEL FOR ORTHOSIS PRESCRIPTION SUPPORT SYSTEMS

Jun Inoue, Kazuya Kawamura, Masakatsu G. Fujie
Tokyo Denki Univ. Dept. of Robotics and Mechatronics
Senju-Asahi-cho 5, Adachi-ku, Tokyo, 120-8551 Japan
inoue.jun@fr.dendai.ac.jp

ABSTRACT

In this paper, we performed biodynamic verification of a muscular activity model using Bayes estimation. In creating this model, we aimed to enable quantitative selection of lower foot orthoses based on a patient's muscular activity in the lower foot. Because physical models require the use of large-scale measurement systems, which cannot be used clinically, they are not suitable for making these measurements. Therefore, we chose Bayes estimation to construct a model for estimating the muscular activity from parameters that can be measured easily, such as joint angle and sole pressure. This model allows for not only the estimation of muscle activity, but also another closely related parameter through the change in muscular activity, which is a parent node to the muscle activity node. The three advantages of our model are that it 1) reports the influences on muscle activity, which change throughout the gait cycle, by using 10% level nodes for each factor; 2) expresses the influence of those factors, which are different at low and high muscular activity levels; and 3) compensates for missed predictions by estimating muscle activity in 10% increments. Here, we verify the biodynamic validity of the model parent node for four foot muscles.

KEY WORDS

Gait Analysis, Lower Leg Orthosis, EMG, Bayesian Network.

1. Introduction

The number of strokes is estimated at 2,000 per million people per year, with a death toll of 900, which constitutes the fourth largest cause of death in the world [1, 2]. Moreover, patients who survive strokes often have physical impediments, such as hemiplegia, and social participation can become difficult. Lower foot orthoses are prescribed to maintain standing position posture or to support walking in patients with leg paralysis.

Various types of lower foot orthoses exist, which can be roughly classified into knee-ankle-foot orthoses and ankle-foot orthosis. Knee-ankle-foot orthoses are prescribed to patients with severe symptoms, such as loss of knee joint stability, disturbance of sensation in the knee circumference, and knee joint deformation. Ankle-foot orthoses are prescribed to patients with symptoms such as

equinovarus foot, decreased stability of a leg joint, the disturbance of sensation below an ankle, and leg joint spasticity. Moreover, because the patients who use ankle-foot orthoses have relatively mild symptoms and the grade of those symptoms can vary, many types of orthoses exist for different symptoms. Several examples are shown in Figure 1.

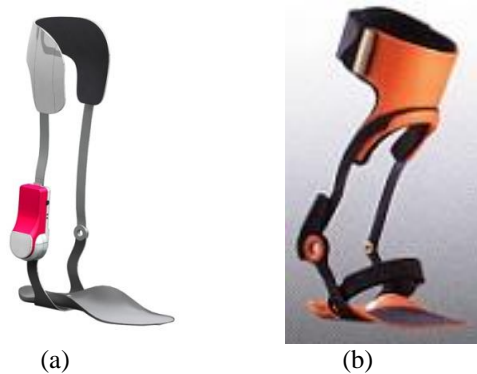


- (a): Articulated plastic ankle-foot orthosis
- (b): Rigid ankle-foot orthosis
- (c): Dream Plastic Ankle-Foot Orthosis
- (d): Double bar ankle-foot orthosis

Figure 1. Variety of lower leg orthoses [5]

Recently, new orthoses using a mechanical engineering design approach have been developed. For example, Furushou *et al.* developed an orthosis with a magnetic fluid damper at the ankle joint [3], and Yamamoto *et al.* developed the “Gait Solution”, which uses a hydraulic brake [4], as shown in Figure. 2. These two new lower foot orthoses have the same aim: to improve viscoelasticity of the ankle joint. Because of flaccid paralysis of a muscle, the lower-limb paretic patient's walking gait has a very short time between heel contact and foot-flat. The viscoelasticity can be improved during plantar flexion with damping, and during dorsiflexion without damping. The important point is that the amount of

necessary support varies over the walking gait cycle, as well as by paretic grade.



(a): An orthosis with a magnetic fluid damper
 (b): The Gait Solution
 Figure 2. New lower leg orthoses [3, 4]

When prescribing orthoses, medical doctors determine paretic grade and muscle strength to decide what kind of orthosis to prescribe. To measure muscle strength, the Manual Muscle Testing technique is generally used. This technique is an examination of a maximum of nine points concerning a patient's muscle strength [6]. The tester presses down on a patient's joint with a constant force and the patient exerts their strength against that power. However, this technique is not generally reproducible between testers, and it is difficult to describe the results quantitatively. As a result, the suitability of an orthosis for a given patient depends on the medical doctor's level of skill. Too little support can cause falls and injuries, while superfluous support can cause loss of muscle strength and decrease range of motion.

We hypothesized that if the amount of patient muscular activity can be estimated based on only patient walking in the clinic, a quantitative model prescribing the best lower foot orthosis could be created to address this problem. A physical model that uses inverse dynamics acts as the main component of our musculoskeletal model in the present work. Delp *et al.* created OpenSim to simulate the whole body [7], and it was developed as an open source platform. Nakamura *et al.* created a whole body muscle model [8] that can estimate and display muscular activity in real time. Takashima *et al.* performed a dynamic model analysis of the human foot [9] that contains the arch joint and one metacarpophalangeal (MP) joint. While these models are high-precision and can be applied to various actions, they require large-scale and expensive equipment, such as a three-dimensional-motion-analysis system and a floor-reaction-force measuring unit, making them difficult to use on patients at the point of care.

Our final objective is to assemble the following orthosis prescription support system. (1) Estimates of muscular activity are made from simple measurements of a patient walking. (2) A medical doctor looks at the suggested result and decides whether the strength of the support is appropriate to assist the muscles that need training. (3) The most suitable lower limb orthosis for the

patient is prescribed based on the strength of the support approved by the medical doctor.

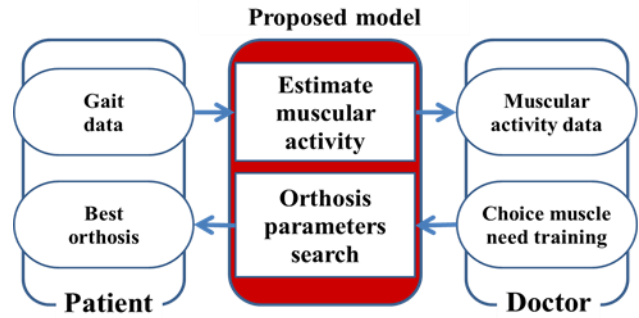


Figure 3. System conceptual diagram

2. Methods

2.1 Approach

In this study, we decided to use parameters that estimate muscular activity defined not using physical models, but with a statistical model. Moreover, after estimating muscular activity, it is necessary to find the cause of the decrease in muscular activity in order to translate the estimate results into an appropriate orthosis selection. That is, a learning requirement exists for the consecutive causality between muscular activity and every other parameter. For this reason, we decided to use a Bayesian network, which is a type of statistical model. The Bayesian network builds a causation model from the joint probability of several phenomena to estimate the probability of the desired phenomenon under a certain condition. As an example in another field, Bayesian estimation can discriminate spam mail by filtering combinations of various words in emails [10].

Even without a physical model, it is necessary to use parameters that have physical meaning and are serially correlated one-to-one with muscular activities during walking. If a patient is restricted to walking, we can assume the timing of the gait cycle from a joint angle. Moreover, since no external force is applied other than at the sole of the foot, we can assume the posture of the upper half of the body based on the distribution of the power at the sole of the foot. Therefore, we decided to estimate the amount of muscular activities using only the angle of the hip, knee, ankle, and a toe joint, and the distribution of pressure on the sole of the foot.

Several researchers have also used Bayesian networks to predict muscular activity [11], though the estimates have not always been accurate. To improve this process, we built the foot muscular activity model with a lower foot orthosis, as shown in Figure 5, and the electromyography (EMG) data from the muscles was divided into ten levels. Usually, when evaluating muscular activity, the maximum voluntary contraction is used. However, there are changes in muscle activities during walking that cannot be easily seen from maximum voluntary contraction data. Thus, we defined the maximum

muscle strength during gait as 100%, and divided that into 10% muscular-activity levels. The angle of each joint and the sole pressure on each part were also divided into ten levels according to the EMG division as shown in Figure 4.

The maximum dorsiflexion angle (Figure 6c) was defined as 0%, and the maximum plantar-flexion angle (Figure 6d) as 100%, and we divided this range into ten levels. Similarly for the knee and hip joints, the maximum extension angle was defined to be 0% and the maximum flexion angle to be 100%, and these ranges were also divided into ten levels. We used these ranges to determine the thresholds and to make nodes for the Bayesian network. This method can classify the influence of different conditions for some of the parameters as either “high” or “low”.

2.2 Model Construction Method

The outline of the algorithm that builds the model from the walking data is shown in Figure 7. From the measurements of the three kinds of data described above, we built a model that represents the relationship between muscular activity, joint angle, and sole-of-foot pressure with the Bayesian network using a synchronous occurrence probability. We used a K2 algorithm for the texture learning, which is a type of greedy search algorithm to assemble the Bayesian network. A greedy search algorithmic is a network construction method that repeatedly adds the parent node to greatly improve the valuation basis as long as the value of the valuation basis improves. Although the K2 algorithm is a type of greedy search algorithm, an additional process can be used that limits parent node candidates for each node based on a prior information or technical knowledge.

Moreover, it is possible that the causes of muscle work differ between the control term, which is in the first half of the stance phase, and the propulsive term, which is in the latter half of the stance-phase. Therefore, when building the model, we further divided the gait cycle into the control term and the propulsive term in the stance phase, and built the model to address them separately, as shown in Figure 8. We have previously evaluated the effectiveness of this divided model method [12].

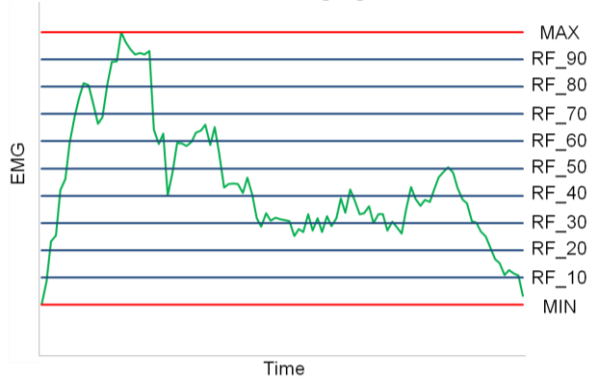
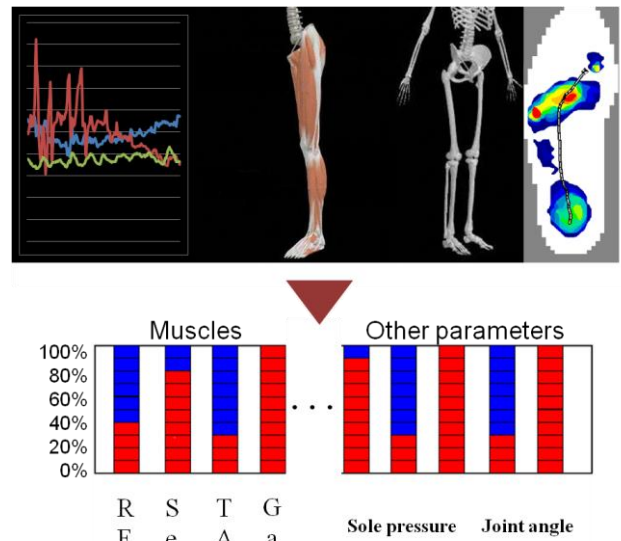


Figure 4. Definition of muscular-activity level



RF: Rectus femoris muscle; Se: Semitendinosus muscle; TA: Tibialis anterior muscle; Ga: Gastrocnemius muscle;

Figure 5. Nodes of the Bayesian Network

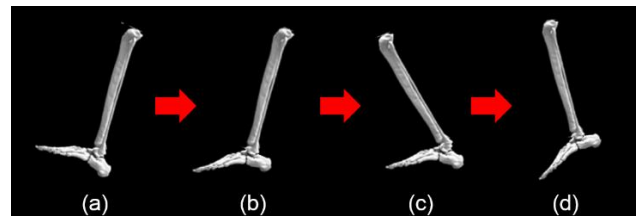


Figure 6. State changes of the ankle joint

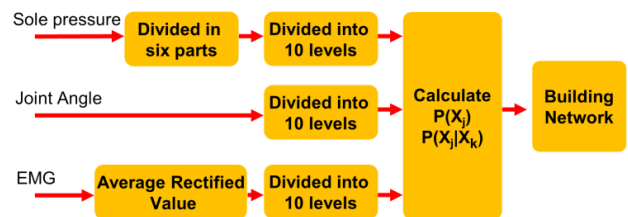


Figure 7. Outline of the model construction method

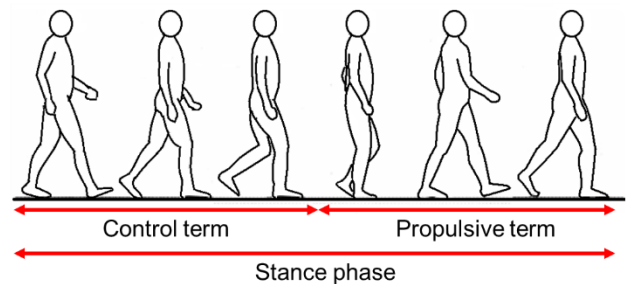


Figure 8. Gait cycle divisions

3. Experiment

3.1 Experimental description and conditions

We measured the foot electromyography, joint angles, and plantar pressure distribution during gait for the purpose of building the muscular-activity estimate model and examining its validity. The test subject was a healthy person in his twenties. Subject walks 8m passage for experiments and if subject stagger or feel wrongness we stop the measurement. (Figure 9)

We made the following measurements on the normal gait:

EMG: (Figure 10)

RF: Rectus femoris muscle; Se: Semitendinosus muscle;
TA: Tibialis anterior muscle; Ga: Gastrocnemius muscle;

Joint Angle: (Figure 11)

A1: Hip joint; A2: Knee joint; A3: Ankle joint; A4, A5, A6: Metatarsophalangeal joints (big toe, 3rd toe, 5th toe)

Sole Pressure: (Figure 11)

P1: Big toe; P2: 5th toe; P3: Thenar eminence; P4: Hypothenar eminence; P5: Outside metatarsus; P6: Calcaneus

Other:

Floor reaction force (for the divided gait cycle)



Figure 9. Measuring situation

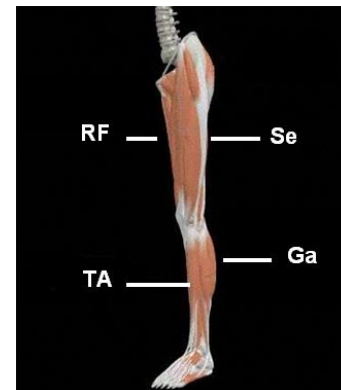


Figure 10. Measured muscles

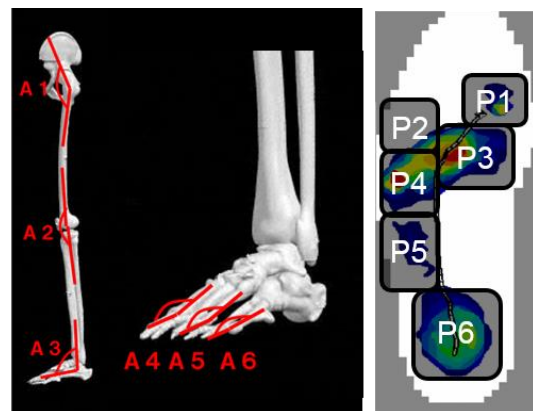
3.2 Results

3.2.1 Quantitative assessment

The results of the model built from the obtained measurements are shown below. The accuracy of the model was verified for every time series following the protocol shown in Figure 7. The estimated accuracy of every four muscles was more than 90 percent. The estimated accuracies for each muscle in both divided and non-divided models are shown in Figure 12. The accuracy of the divided model was more than 95% for all muscles studied.

3.2.2 Qualitative assessment

Next, the parent node for every activity level of each muscle were calculated. The results of the following four muscles are shown in Tables 1 and 2: Rectus femoris, Semitendinosus, Tibialis anterior, and Gastrocnemius. The result of the control term is shown in Table 1, and the result of the propulsive term is shown in Table 2. The left side of the tables is divided into 10% increments for every activity level of each muscle. The right is a deep relation measurement parameter for each muscle activity level, including primary, secondary, and tertiary parent nodes, sequentially from the left.



left: Joint measurements
right: The divisions of the sole.
Figure 11. Measured positions

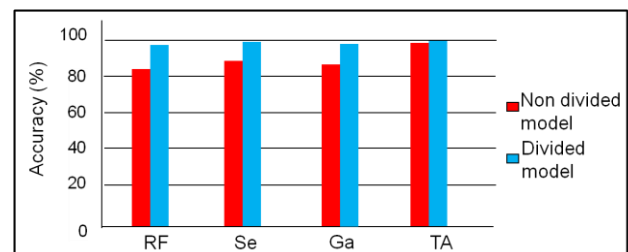


Figure 12. Comparison of model accuracy

Table 1 Parent nodes for each muscle activity level in the control term

	Primary parent node	Secondary parent node	Tertiary parent node		Primary parent node	Secondary parent node	Tertiary parent node
RF_90				Se_90	A3_90		
RF_80	A3_80			Se_80	A3_90	A4_90	
RF_70	A3_80	P6_70	A2_80	Se_70	A3_90	A1_20	
RF_60	A3_80	P5_40	P3_10	Se_60	A3_90	A5_20	A3_50
RF_50	A3_80	A1_20	P5_40	Se_50	A6_30	A3_90	A1_20
RF_40	A1_20	P5_60	A3_80	Se_40	P5_20	P2_10	P5_60
RF_30	A1_40	A3_70	P2_10	Se_30	A6_50	P4_40	A2_80
RF_20	A1_40	P3_40	P2_10	Se_20	P4_50	A5_90	A2_80
RF_10	A1_40	A1_60	P3_30	Se_10	P5_90	A6_90	A2_80
	Primary parent node	Secondary parent node	Tertiary parent node		Primary parent node	Secondary parent node	Tertiary parent node
TA_90	A3_90			Ga_90	A6_90		
TA_80	A3_90	A2_90		Ga_80	A6_90	A3_70	
TA_70	A3_90	A5_70	A6_10	Ga_70	A6_90	A1_20	
TA_60	A4_90	P4_10	P5_10	Ga_60	A6_90	P4_20	P5_20
TA_50	A4_90	P4_10	A5_70	Ga_50	A6_90	P4_20	P5_10
TA_40	A4_90	A3_80	A5_60	Ga_40	A6_90	P4_20	A6_50
TA_30	P3_10	A1_20	A2_80	Ga_30	A6_90	P4_20	A2_90
TA_20	A1_20	P6_90		Ga_20	P6_90	P3_20	A2_90
TA_10	P4_20	A1_10		Ga_10	A6_40	P5_20	A1_20

Table 2 Parent nodes for each muscle activity level in the propulsive term

	Primary parent node	Secondary parent node	Tertiary parent node		Primary parent node	Secondary parent node	Tertiary parent node
RF_90	P2_90			Se_90			
RF_80	P2_70	A3_10		Se_80			
RF_70	A1_90	P2_70		Se_70			
RF_60	A1_90	P2_60	P3_90	Se_60			
RF_50	A1_90	P3_90	P2_70	Se_50			
RF_40	A3_10	P3_50	P2_60	Se_40			
RF_30	P4_90	P1_30		Se_30	A5_60	A4_10	A3_70
RF_20	P3_20	P4_90		Se_20	A5_60	A2_40	A6_10
RF_10	P4_90	P4_30		Se_10	A5_70	A1_40	P3_50
	Primary parent node	Secondary parent node	Tertiary parent node		Primary parent node	Secondary parent node	Tertiary parent node
TA_90				Ga_90			
TA_80				Ga_80	P1_90	P2_70	
TA_70				Ga_70	P1_70	A4_40	P2_60
TA_60				Ga_60	P4_70	P6_80	P1_80
TA_50				Ga_50	P4_70	P6_80	A6_10
TA_40				Ga_40	P4_70	A6_10	P6_80
TA_30	A3_90			Ga_30	P4_70	A6_10	P2_60
TA_20	A2_10			Ga_20	P3_20	P4_80	A6_10
TA_10	A1_90	P5_60	P1_20	Ga_10	P3_90	P5_70	P4_60

3.3 Discussion

The primary parent node expresses the main biodynamic features. These are reported below with descriptions comparing the results and the actual movements of each muscle in the control and propulsive terms to discuss the biodynamic features.

Control term: Rectus femoris muscle

The primary parent nodes show that the 80% node of the ankle joint (A3) strongly influenced the 50% node to the 80% node of the Rectus femoris muscle activity level. This shows that the muscle activity level is higher during the stretch from 50% to 80% in a working muscle at the same time as the ankle joint extends to 80% of the maximum extension. This result suggests that the rectus femoris muscle works rapidly during actual gait after each foot-flat in order to speed the body forward.

Control term: Semitendinosus muscle

The primary parent nodes show that the 90% node of the ankle joint (A3) strongly influenced the 60% to 90% nodes of muscle activity level. This shows that increased activity levels during a stretch from 60% to 90% at the same time as the ankle joint extends to almost the maximum expansion. This result suggests that the timing of Semitendinosus muscle work is slightly earlier than the Rectus femoris muscle, and this work is in order to speed the body forward.

Control term: Tibialis anterior muscle

The primary parent nodes show that the 90% node of the ankle joint angle (A3) strongly influenced the 70% to 90% muscle activity nodes. The main work of the Tibialis anterior is suppressing the rapid expansion of the ankle joint just before the foot-flat after heel grounding occurs during gait in the first half of the control term. Thus, this result agrees with how actual muscles roll.

Control term: Gastrocnemius muscle

The primary parent node shows that the 90% node of the 5th toe angle (A6) influenced the 30% to 90% muscle activity nodes. Moreover, the secondary parent node shows that the 20% node of the sole pressure on the hypothenar eminence (P4) influenced the 30% to 60% of muscle activity. These results suggest that the roll of the Gastrocnemius muscle works to prevent knee bending when the sole pressure distribution begins moving towards the hypothenar eminence during the last half of the control term.

Propulsive term: Rectus femoris muscle

The primary and secondary parent nodes show that the 60%, 70%, and 90% sole pressure nodes on the 5th toe (P2) influenced muscle activity from 60% to 90%. This shows that muscle activity reaches a peak as the bottom pressure of the small toe increases at 60%, 70%, and 90%. During actual walking, when generating power on the 5th toe and beginning to kick the ground as the last step of the

propulsive term, this indicates that the rectus femoris muscle is working.

Propulsive term: Semitendinosus muscle

No parent node was observed in nodes at less than 40% of muscle activity. This shows that the Semitendinosus muscle is mostly not working during the propulsive term. This agrees with the idea that the Semitendinosus muscle works strongly when pushing the body ahead during the control term in actual walking.

Propulsive term: Tibialis anterior muscle

No parent node was observed in nodes at less than 40% of muscle activity. This shows that the Tibialis anterior muscle is not working during the propulsive term. This agrees with the idea that the Tibialis anterior prevents the ankle joint from extending suddenly in the control term, and does nothing in the propulsive term.

Propulsive term: Gastrocnemius muscle

The primary parent node shows that the 70% node of the sole pressure on the hypothenar eminence (P4) influenced from 30% to 60% of the muscle activity, and the 70% and 90% nodes of the sole pressure on the big toe (P1) has influenced from 80% to 90% of muscle activity. This suggests that when 70% of the maximum overlying pressure is on the hypothenar eminence, the muscle activity will begin to increase, and when the sole pressure on the big toe is close to the maximum overlying pressure, the muscle activity is also near its maximum. This agrees with the idea that the gastrocnemius engages to kick the ground by putting pressure on the hypothenar eminence of the big toe during the latter half of the propulsive term in actual walking.

4. Conclusion

In this paper, we performed qualitative verification of a muscle activity estimation model that used a Bayesian network. We created this model to assist in the prescription of lower extremity support orthoses. Therefore, the model should be able to express causal relationships with high estimated accuracy. The parent nodes obtained for four muscles were used to verify whether their motion was biodynamically meaningful as a qualitative check. The results indicate that the parent nodes of the muscles in the model reflect the motion of those muscles during gait. For further research, we increase subjects and build a model applicable to people who class as various group like as male, female, the child or the aged.

Acknowledgements

This work is supported in part by a grant from the Moritani Scholarship Foundation and by the Global COE (Centers of Excellence) Program "Global Robot Academia," in part by a Grant for Scientific Research (A) (90198664) from the Ministry of Education, Culture, Sports, Science and

Technology of Japan, and in part by a Grant-in-Aid for Research Activity Start-up Grant Number (25882031).

References

- [1] World Health Organization., *The world health report 2003*"Chapter1, pp.12-20.< <http://www.who.int/whr/2003/en/index.html>>.Accessed 2014 Jan 15.
- [2] Leys D, Atherothrombosis: a major health burden, *Cerebrovasc Dis.* 2001. Suppl 2, 1-4
- [3] Tanida Sousuke, Kikuchi Takehito, Furusho Junji, Ozawa Takuya, Ostuki Kikuko, Fujikawa Takamitsu, Morimoto Shoji, Hashimoto Yasunori, Yasuda Takashi, The development and clinical evaluation of an intelligent ankle foot orthosis using compact type MR fluid brakes *Journal of the Society of Biomechanisms* 34(2), 124-131, 2010-05-01
- [4] S. Yamamoto, A. Hagiwara, T. Mizobe, O. Yokoyama, and T. Yasui,Development of an ankle-foot orthosis with an oil damper, *Prosthet.Orthot. Int.*, vol. 29, pp. 209–19, Dec. 2005.
- [5] Japan Orthotics Prosthetics Association , *Catalog of prosthetic limb and orthosis (in Japanese)*
- [6] Helen J. Hislop, Jacqueline Montgomery, *Daniels and Worthingham's Muscle Testing: Techniques of Manual Examination*
- [7] Delp SL, et al. OpenSim: open-source software to create and analyze dynamic simulations of movement. *IEEE Trans. Biomed. Eng.* 2007;54:1940–1950.
- [8] Y. Nakamura, K. Yamane, Y. Fujita, and I. Suzuki,somatosensory computation for man-machine interfacefrom motion capture data and musculoskeletal humanmodel, *IEEE Transactions on Robotics*, Vol. 21(1), pp. 58-66, 2005.
- [9] T.Takashima,H.Fujimoto,W.Kakihata,A, Takanishi “ Model Analysis of the Human Foot Include Subtalar Joint,Taroclural Joint, Taroclural Joint, and Foot Arch” *Transactions of the Japan Society of Mechanical Engineers. C*, Vol.69, No.688, 111-116, 2003
- [10] Subramaniam, T., Jalab, H.A., Taqa, A.Y.” Overview of textual anti-spam filtering techniques” *International Journal of Physical Sciences*, Volume 5, Issue 12, pp. 1869-1882,4 October 2010
- [11] L A Johnson, and A J Fuglevand, Evaluation of probabilistic methods to predict muscle activity: implications for neuroprosthetics, *J Neural Eng.* 2009
- [12] Jun Inoue, Kazuya Kawamura, Masakatsu G. Fujie, Developing an ankle-foot muscular model using Bayesian estimation for the influence of an ankle foot orthosis on muscles , *Proc.The Fourth IEEE RAS/EMBS International Conference on Biomedical Robotics and Biomechatronics* Roma, Italy,2012,431-436